Phys. Status Solidi RRL 5, No. 1, 1–9 (2011) / DOI 10.1002/pssr.201004371

pss +++rapid research letters+++
www.pss-rapid.com

Review@RRL

Competing energy scales in high-temperature superconductors: Ultrafast pump–probe studies

Elbert E. M. Chia[*,1], Jian-Xin Zhu[2], D. Talbayev[3], and A. J. Taylor[2]

[1] Division of Physics and Applied Physics, School of Physical and Mathematical Sciences, Nanyang Technological University, Singapore 637371, Singapore
[2] Los Alamos National Laboratory, Los Alamos, NM 87545, USA
[3] Department of Chemistry, Yale University, P.O. Box 208107, New Haven, CT 06520-8107, USA

Received 24 August 2010, revised 18 November 2010, accepted 19 November 2010
Published online 29 November 2010

Keywords superconductivity, time resolved spectroscopy, optical properties, magnetic properties, pnictide superconductors, cuprate superconductors

[*] Corresponding author: e-mail elbertchia@ntu.edu.sg, Phone: +65-6513-8132, Fax: +65-6795-7981

We present a review of photoexcited quasiparticle dynamics of cuprate and pnictide high-temperature superconductors in regimes (temperature, doping) where different phases such as superconductivity, spin-density-wave (SDW) and pseudogap phases coexist or compete with one another. We start with the overdoped cuprate superconductor $Y_{1-x}Ca_xBa_2Cu_3O_{7-\delta}$, where the superconducting gap and pseudogap coexist in the superconducting state. In another cuprate $Tl_2Ba_2Ca_2Cu_3O_y$, we observe a competition between SDW and superconducting orders deep in the superconducting state. Finally, in the underdoped iron pnictide superconductor $(Ba,K)Fe_2As_2$, SDW order forms at 85 K, followed by superconductivity at 28 K. We also find the emergence of a normal-state order that suppresses SDW at a temperature $T^* \sim 60$ K and argue that this normal-state order is a precursor to superconductivity.

1 Introduction In recent years, femtosecond time-resolved spectroscopy has been recognized as a powerful *bulk* technique to study temperature (T)-dependent changes of the low-lying electronic structure of superconductors and other strongly correlated electron materials [1–3]. It provides a new avenue, namely the time domain, for understanding the quasiparticle (QP) excitations of a material. It was used, for example, to determine the magnitude of the electron–phonon coupling constant of conventional superconductors [4, 5], uncouple the dynamics of the superconducting (SC) and pseudogap phases (for example, [6]), and determine the bare QP recombination rate [7]. Reviews exist that survey the use of time-resolved methods such as all-optical pump–probe, terahertz time domain spectroscopy (THz-TDS), and optical pump–THz probe (OPTP) spectroscopy, in the study of strongly correlated materials (see, for example, [1] and [2]). Recently, the exciting technique of time-resolved angle-resolved photoelectron spectroscopy (TR-ARPES) was used to study the dynamics of photoexcited electrons in optimally-doped $Bi_2Sr_2CaCu_2O_{8+\delta}$, and concluded that 20% of the total lattice modes dominate the coupling strength between electrons and phonons, with the electron–phonon coupling constant $\lambda < 0.25$ [8]. Also, the coupling strength between fermionic quasiparticles and spin fluctuations (another type of bosons like phonons) was recently estimated from a consistent description of time-integrated ARPES and inelastic neutron scattering data on the high-temperature superconductor (HTSC) $YBa_2Cu_3O_{6.6}$ [9]. This shows that time-resolved and time-integrated techniques of the same type complement each other in answering important questions regarding the mechanism of high transition temperature (T_c) superconductivity.

Ultrafast techniques, however, have largely been used to study single phases in superconductors. In materials where different order parameters coexist or compete with one another, photoexcited electrons couple differently to these degrees of freedom (such as charge, lattice, spin, orbital). These photoexcited electrons thus relax via different pathways, and this shows up as multi-component relaxa-

tion in the raw data, with different relaxation times. In this Review, we present time-resolved studies of photoexcited QP dynamics in HTSCs where superconductivity coexists with long-range orders such as the pseudogap phase, the antiferromagnetic (AFM) (or spin density wave, SDW) phase, or both. In the cuprate HTSC $Y_{1-x}Ca_xBa_2Cu_3O_{7-\delta}$ (Y-123) [6], there is evidence of the coexistence of the SC gap and pseudogap in the SC state. In the tri-layered cuprate HTSC $Tl_2Ba_2Ca_2Cu_3O_y$ (Tl-2223, $T_c = 115$ K) [10] we observe that its pristine SC state ($40\ \text{K} < T < T_c$) subsequently evolves into a coexistence phase (of superconductivity and AFM phase) as evidenced by a strong modification of the gap dynamics below 40 K. In the pnictide HTSC $(Ba,K)Fe_2As_2$ (BKFA) [11] the situation is more complicated: in the underdoped sample, three energy scales exist – SDW (at Néel temperature $T_N \sim 85$ K), superconductivity (at $T_c \sim 28$ K) and a normal-state phase (at $T^* \sim 60$ K). This normal-state phase smoothly evolves into the SC phase, and at the same time suppresses the SDW phase. We attribute this normal-state phase to the emergence of precursor superconductivity. The data from BKFA are also consistent with the notion of phase separation in these materials. This Review shows that, not only are ultrafast techniques very useful in discerning the existence of different phases in the material, they can also tell us whether one phase (such as superconductivity) merely coexists, or *competes* with another phase in close proximity (such as SDW phase). We only discuss data taken from the all-optical pump–probe setup, since other techniques, such as time-resolved THz and photoemission, have not yet begun to explore the issue of competing orders in superconductors.

2 Experimental technique An ultrafast pump–probe setup employs sub-100 fs optical pump pulses to photoexcite QPs in a material. The subsequent evolution and relaxation of QPs is monitored by measuring the changes in material's reflectance (or transmittance) by time-delayed probe pulses. The probe pulses are usually at least 10 times weaker than the pump pulses. A train of pulses from a femtosecond laser is split into pump and probe parts by a beamsplitter, and the time delay between pump and probe is achieved via a longer propagation path for the probe beam (a 1 cm path difference corresponds to 33.3 ps time delay). Typical pump–probe data on a metal are shown in Fig. 2(a), the $T = 80$ K curve. The pump pulse hits the surface of the material at time $t = 0$ ps, and a sharp change (a sharp rise in Fig. 2(a)) in the material's photoinduced reflectance ($\Delta R/R$) is observed. The rise time in $\Delta R/R$ is usually the result of QP population buildup competing with the decay of QPs, but sometimes it is a coherent artifact. The subsequent decay of $\Delta R/R$ indicates the relaxation of photoexcited QPs to equilibrium population.

Pump–probe studies of superconductors reviewed here were carried out in a low-excitation regime with photoinduced QP density of ~0.001/unit cell. Such low excitation density is achieved by using 0.3–1 mW of average power from an 80 MHz repetition rate Ti:sapphire laser operating at 800 nm wavelength (1.55 eV) and focusing the pump and probe pulses down to 60 μm and 30 μm spots, respectively. The small spot sizes minimize sample heating by the pump, which is typically ~10 K at the lowest T and is accounted for in all data presented here. The sensitivity in $\Delta R/R$ of at least 1 part in 10^6 was achieved by modulating the pump beam at 1 MHz with an acoustic-optical modulator.

QP relaxation in a normal metal is governed by electron–electron (e–e) and electron–phonon (e–ph) scattering. At high T, e–e scattering proceeds much faster than e–ph scattering. The photoexcited QP distribution thermalizes through e–e scattering within tens of femtoseconds, and after that the e–ph scattering allows the equilibration electronic and lattice temperatures [12]. This e–ph relaxation manifests as a decay of photoinduced $\Delta R/R$ on a picosecond (ps) time scale. The decay is well described by a single-exponential decay function $\Delta R/R = A \exp(-t/\tau)$, where A and τ are fitting parameters. The amplitude A is proportional to the photoexcited QP density, whereas the relaxation time τ corresponds to e–ph relaxation and is related to the e–ph coupling constant λ [4], which allows the measurement of λ in conventional superconductors by measuring τ in their normal state at room temperature [5].

In superconductors and many other correlated electron materials, many-body interactions open a gap in the QP density of states, thereby introducing an additional timescale for the QP dynamics. Independent of its origin, the opening of a gap presents a bottleneck to ground state recovery following photoexcitation of QPs across the gap. This bottleneck results in a quasidivergence of the relaxation time near T_c. Figure 1 illustrates the origin of this quasidivergence. After the initial fast e–e thermalization, the QPs reside on the gap edge. They can recombine to form Cooper pairs and emit a high-frequency phonon (HFP) (with energy $\omega > 2\Delta$, where Δ is the gap magnitude). If these HFPs remain in the system, they can break Cooper

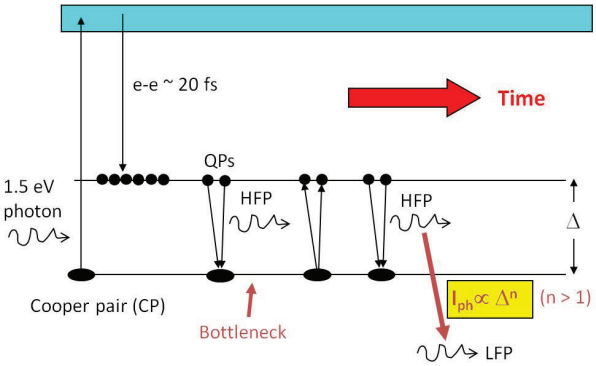

Figure 1 (online colour at: www.pss-rapid.com) Schematic to explain the quasi-divergence of the relaxation time near T_c, when a gap opens up in the density of states. I_{ph} is the scattering integral for the processes where the HFPs decay or inelastically scatter to become LFPs.

pairs to create more QPs, thus slowing down the (energy) relaxation of the QPs in the system.

However, if these HFPs manage to lose their energy (via processes described in the next section) to form low-frequency phonons (LFP) ($\omega < 2\Delta$), then these LFPs will not have enough energy to break any Cooper pairs. The rate at which the HFPs lose their energy increases with the gap magnitude [13]. As temperature decreases, the gap magnitude increases, thus the population and energy of the QPs decrease (i.e. relax) faster, causing a shorter relaxation time. This explains the quasi-divergence of the relaxation time as T approaches T_c from below. Interactions which perturb the gap thus manifest as an easily measured change in the temporal response by monitoring changes in $\Delta R/R$ (or transmission) of an interrogating probe beam. This effect was first considered by Rothwarf and Taylor [14]. Their description of QP relaxation in a superconductor is now known as the Rothwarf–Taylor model.

3 Rothwarf–Taylor model The Rothwarf–Taylor (RT) model is a phenomenological model that was used to describe the relaxation of photoexcited superconductors [7, 14], where the presence of a gap in the electronic density of states gives rise to a relaxation bottleneck for carrier relaxation. When two QPs with energies $\geq\Delta$ recombine, a HFP is created. The HFPs released in the QP recombination are trapped within the excited volume and can further re-break Cooper pairs; hence they act as a bottleneck for QP recombination, and recovery of superconductivity is governed by the decay of the HFP population. The evolution of QP and HFP populations is described by a set of two coupled nonlinear differential equations. The RT model has also been applied to the study of heavy fermions, where the dynamics are associated with a gap resulting from the hybridization of the conduction electrons with the localized f-levels [15].

The results of the RT model are as follows [2, 16]: From the amplitude $A(T)$, one obtains the density of thermally excited QPs n_T via the relation

$$n_T(T) \propto \mathcal{A}(T)^{-1} - 1, \tag{1}$$

where $\mathcal{A}(T)$ is the normalized amplitude, $\mathcal{A}(T) = A(T)/A(T \to 0)$. Then, from the QP density [13]

$$n_T(T) \propto \sqrt{\Delta(T)T}\,\exp\left(-\Delta(T)/T\right), \tag{2}$$

one obtains Δ_0, the zero-temperature gap. Moreover, for a constant pump intensity, the T-dependence of n_T also governs the T-dependence of τ^{-1}, given by

$$\tau^{-1}(T) = \Gamma[\delta(\beta n_T + 1)^{-1} + 2n_T]\,(\Delta + \alpha T \Delta^4), \tag{3}$$

where Γ, δ, β, and α are T-independent fitting parameters. The term $[\Delta(T) + \alpha T \Delta(T)^4]$ in Eq. (3) accounts for the T-dependence of the phonon decay rate. It arises from the fact that HFPs lose their energy to become LFPs via two processes [13] – (i) the inelastic scattering of a HFP with the creation of one LFP, and (ii) the decay of one HFP to two LFPs. These LFPs then will not be able to participate in Cooper pair breaking to create more QPs, resulting in a faster relaxation of the QPs in the system. The first process yields $\tau^{-1}(T) \propto \Delta(T)$, while the second gives $\tau^{-1}(T) \propto T\Delta(T)^4$. This factor ensures that the values of Δ_0 obtained from fits to $A(T)$ and $\tau(T)$ are the same [17].

4 Data and analysis

4.1 $Y_{1-x}Ca_xBa_2Cu_3O_{7-\delta}$ (Y-123) Many hole-doped cuprate HTSCs exhibit an unusual normal state that is characterized by the opening of a gap in the electronic spectrum, at a temperature T^* above T_c. Much theoretical and experimental effort has been spent in ascertaining the origin of this gap, called the pseudogap [18], for the answer may prove crucial in the understanding of high-temperature superconductivity. A fundamental issue regarding the pseudogap phase is [19]: Does it compete with, is unrelated to, or is a precursor of, superconductivity? Related to this is the number of energy gaps below T_c: A single energy gap would imply that the pseudogap is a precursor state, while two gaps would suggest that the pseudogap is a competing or a coexisting phase [20].

In Ref. [6] experiments were performed on four Y-123 single crystals with x = 0, 0.016, 0.101, and 0.132 and T_c's of 93, 89.5, 83 and 75 K, respectively, grown by the self-flux method. In this Review we will only show data from the x = 0.132 sample. The time evolution of $\Delta R/R$ is shown in Fig. 2(a). Above T_c, a single exponential gives a very good fit to the data, with a relaxation time of ~0.5 ps. *Below* T_c, however, there are now *two* relaxation times, one with $\tau_B \approx 0.5$ ps and the other with $\tau_A \approx 3$ ps. In the logarithmic plots shown in Fig. 2(b), this is more clearly shown as a break in the slope near t = 3 ps. A two-component fit was used to fit the data: $\Delta R/R(t) = A(T)\exp(-t/\tau_A) + B(T)\exp(-t/\tau_B)$.

Figure 2(c) shows the relaxation times τ_A and τ_B as a function of T. Notice the divergence of τ_A just below T_c. In contrast, τ_B is completely T independent. The divergence of τ_A at T_c is evidence for the opening up of a T-dependent gap $\Delta_c(T)$ – by "T-dependent" gap we mean a gap that changes with temperature and vanishes at T_c. The simultaneous presence of a T-independent τ_B indicates the *coexistence* of a T-independent gap Δ_p. Using the fact that the energy of the initial pump pulse must be distributed among the electrons and phonons, the authors obtained expressions for the T-dependence of the photoexcited amplitude due to both types of gaps, and from the data fit obtained values of $\Delta_c(0)$ and Δ_p. It is evident from the plot that the total amplitude $|\Delta R/R|$ can be described accurately only by a two-component fit and cannot be described by either component separately. If we associate Δ_c to the SC gap and Δ_p to the pseudogap, then data on Y-123 show the coexistence of the SC and pseudogap phases below T_c, thus validating the "two-gap" scenario. It must be pointed out, however, that the authors of [6] attributed the existence of the two different components to the presence of spatially in

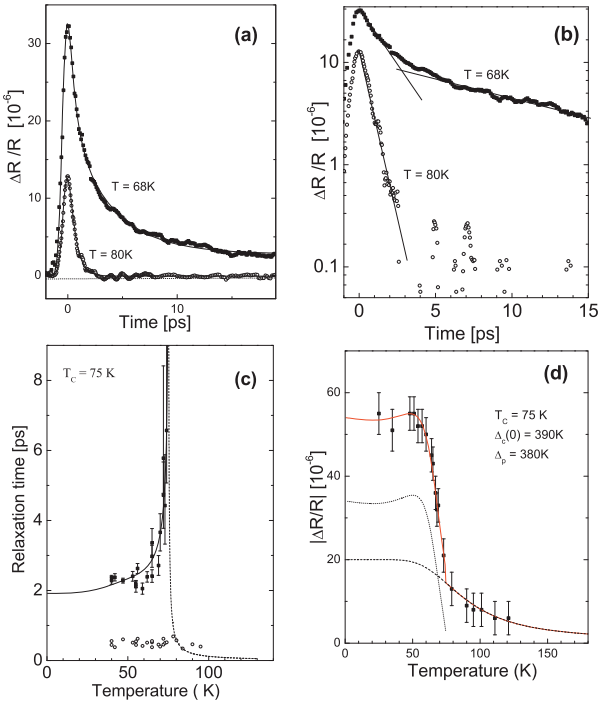

Figure 2 (online colour at: www.pss-rapid.com) (a) Photoinduced reflection $\Delta R/R$ of Y-123 above and below T_c as a function of time for $x = 0.132$ ($T_c = 75$ K). (b) Same data as in (a), but presented on a logarithmic scale. (c) The relaxation times τ_A (squares) and τ_B (open circles) as a function of T. The solid and dashed lines are fits by theoretical expressions given in Ref. [6]. (d) Photoinduced reflection amplitude, $|\Delta R/R|$, as a function of T for the same sample. The fits are made using the sum of Eqs. (2) and (3) of Ref. [6]. The values of $\Delta_c(0)$ and Δ_p used in the fit are shown. The separate $A(T)$ and $B(T)$ are also shown as a dotted line and a dashed line, respectively (reproduced with permission from [6], http://link.aps.org/abstract/PRL/v82/p4918). Copyright 1999 by the American Physical Society.

homogeneous ground state. Another important pump-probe paper on stoichiometric $YSr_xBa_{2-x}Cu_4O_8$ (Y-214) ($x = 0$, 0.4) [21] showed that the two components have different probe polarization dependencies, and could thus be much better disentangled than the case of overdoped Y-123.

4.2 $Tl_2Ba_2Ca_2Cu_3O_y$ (Tl-2223) In the Bardeen–Cooper–Schrieffer (BCS) theory of superconductivity, which describes the mechanism of conventional superconductivity for conventional metals, electrons form Cooper pairs mediated by the vibrations of the crystal lattice. For the HTSCs, another possibility exists, namely, Cooper pairing via AFM spin fluctuations [22, 23]. Indeed, a full-fledged AFM order, out of which such AFM fluctuations emerge, can also compete with superconductivity as the dominant ground state resulting in uniform [24–26] or inhomogeneous [27] phase coexistence. The coexistence of AFM ordering with superconductivity has been observed in single- or double-layered cuprate systems in the presence of a magnetic field via neutron scattering [25, 28], or in five-layered cuprate systems in zero field using nuclear magnetic resonance (NMR) [26, 29]. However, from these measurements, it is not well understood how the emergence of AFM order affects the QP excitations, which determine the optical and electronic properties of the material.

The sample is a slightly underdoped single crystal of Tl-2223 with $T_c = 115$ K, grown by the self-flux method [30]. Tl-2223 is a tri-layered crystal, where its two outer CuO_2 planes have a pyramidal coordination with an apical oxygen, while the inner plane has a square coordination with no apical oxygen. Figure 3 shows the time dependence of the photoinduced signal of Tl-2223. At high T the signal is characterized by a negative $\Delta R/R$ transient which relaxes within $\tau_n \sim 0.5$ ps (Fig. 3(a)) consistent with QP thermalization in conventional metals [12]. Below T_c, we observe the onset of a positive $\Delta R/R$ with a relaxation time (τ_{SC}) of a few ps due to the opening of the SC gap (Fig. 3(a)). Surprisingly, below ~40 K, $\Delta R/R$ first goes positive, relaxes to zero with a lifetime τ_{SC}, *then crosses zero and goes negative*, before relaxing back to equilibrium over a time scale of a few hundred ps (Fig. 3(b)). We ascribe the short-decay positive signal to the QP relaxation across the SC gap following photoexcitation, and the *long-decay negative signal to a new competing order other than superconductivity*. We attribute this competing order to the AFM order, with transition temperature T_N. Accordingly, we fit the data of $\Delta R/R$ in different T ranges as follows: In the normal state ($T > T_c$), the data follow $\Delta R/R = B_0 + B_n \exp(-t/\tau_n)$, where $B_n < 0$; in the phase with only the SC order parameter ($T_N < T < T_c$), the data follow $\Delta R/R = A_0 + A_{SC} \exp(-t/\tau_{SC})$, where $A_{SC} > 0$; in the coexistence region ($T < T_N$), the data follow $\Delta R/R = A_0 + A_{SC} \exp(-t/\tau_{SC}) + A_{AFM} \exp(-t/\tau_{AFM})$, where $A_{SC} > 0$ and $A_{AFM} < 0$. Figure 4(a) shows the T-dependence of the peak amplitudes $A_{SC}(T)$, $A_{AFM}(T)$ and $B_n(T)$. We see that below ~40 K, A_{AFM} increases from zero, while A_{SC} exhibits a sharp kink.

We first consider the competing AFM component below T_N. In this regime we have two types of ordering – AFM and SC order. The formation of the AFM order opens an isotropic QP gap. Therefore, the bottleneck effect

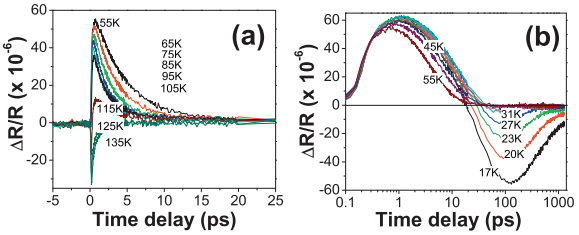

Figure 3 (online colour at: www.pss-rapid.com) Photoinduced transient reflection $\Delta R/R$ versus time delay between pump and probe pulses, of Tl-2223, at a series of temperatures through T_N and T_c (reproduced with permission) from [10], http://link.aps.org/abstract/PRL/v99/i14/e147008). Copyright 2007 by the American Physical Society.

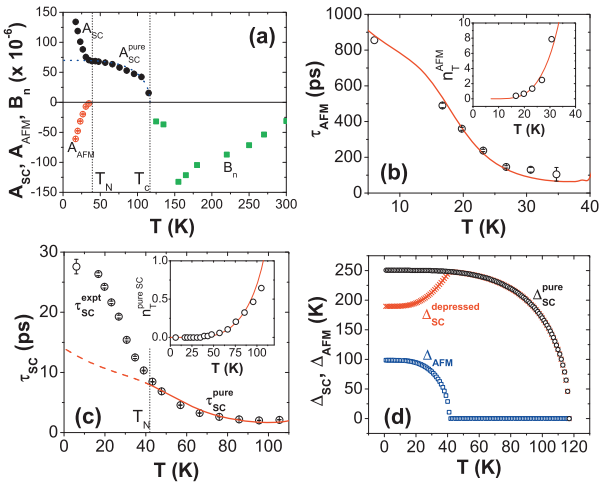

Figure 4 (online colour at: www.pss-rapid.com) (a) T-dependence of the peak amplitudes of Tl-2223. Solid circles: A_{SC}. Open circles: A_{AFM}. Solid squares: B_n. Dotted line: BCS fit to A_{SC} in the T range $T_N < T < T_c$, extrapolated to $T = 0$. (b) $A_{AFM}(T)$ and $n_T(T)$ of the competing order component. Solid curves are fits using the RT model. (c) $\tau_{SC}(T)$ and $n_T(T)$ of the SC component. Solid curves are fits using the RT model. The RT model fit to $\tau_{SC}(T)$ is only for $T_N < T < T_c$ (solid line). The dashed line is the extrapolation of that fit below T_N. (d) SC gap $\Delta_{SC}(T)$ with and without suppression, and the gap $\Delta_{AFM}(T)$ due to the competing order, using the Ginzburg–Landau theory. Adapted from Ref. [10].

is mostly dominated by this new gap. The Ginzburg–Landau free energy for this two-component system is, in a similar fashion to Ref. [31], given by

$$f = \alpha_1\left(1-\frac{T}{T_{c0}}\right)|\Delta_{SC}|^2 + \alpha_2\left(1-\frac{T}{T_{N0}}\right)M^2 + \beta_1|\Delta_{SC}|^4 + \beta_2 M^4 + \beta_3|\Delta_{SC}|^2 M^2 \,. \quad (4)$$

In this expression T_{c0} and T_{N0} are the SC transition temperature of the SC phase, and the Néel temperature of the AFM phase, respectively, *in the absence of the other phase*, whereas the last term indicates a coupling between the two phases. Using this expression for the free energy enables us to compute the T-dependence of the SC gap $\Delta_{SC}(T)$ and the AFM gap $\Delta_{AFM}(T)$ for a given combination of the coefficients α and β. Using the RT model described in the previous section, we obtained good fits to the data for the AFM order (A_{AFM} and τ_{AFM}), using the gap values $\Delta_{AFM}(T)$ obtained from Ginzburg–Landau theory shown in Fig. 4(d). The excellent fit lends strong support to our assumption of the opening of a QP gap upon the development of the competing order. The dynamics of this competing order can be explained by a relaxation bottleneck associated with the presence of a gap in the density of states.

Next we turn to the SC component. In the range $T_N < T < T_c$, with only SC order in the system, we fit the data to the single-component RT model described above, where recombination occurs only from the SC energy gap. The signal amplitude is labeled $A_{SC}^{pure}(T)$, shown in Fig. 4(a), with the superscript denoting the pure SC component without the existence of the AFM order. Using the RT model one obtains $n_T^{pureSC}(T)$ as shown in the inset of Fig. 4(c) (circles), where the fit to Eq. (2) yields $\Delta(0) = 2.14 k_B T_c$ (solid line), in agreement with the typical d-wave value. Again, using these fitted values of $n_T^{pureSC}(T)$, one fits the experimental values of $\tau_{SC}^{pure}(T)$ in the range $T_N < T < T_c$ using Eq. (3), shown in Fig. 4(c). Similar to the competing phase above, the relaxation dynamics of the pure SC phase can also be explained by the presence of a relaxation bottleneck due to a (SC) gap in the density of states.

Notice immediately from Fig. 4(c) that below T_N, the fitted values of $\tau_{SC}^{pure}(T)$ (dashed line) *underestimate* the experimental values. In the Ginzburg–Landau theory, the coupling between the competing and SC order parameters (last term of Eq. (4)) causes the SC gap to be suppressed. Hence the SC energy gap Δ_{SC} decreases below its BCS value, as shown in Fig. 4(d). Since at a fixed T, τ increases as Δ decreases (and vice versa) (see Eq. (3)), we can infer that, below T_N, the increase of the experimental relaxation time $\tau_{SC}^{expt}(T)$ over its BCS value $\tau_{SC}^{pure}(T)$ is due to the *suppression* of the SC gap in this T range. It suggests, once again, the *competing* nature of this AFM order below T_N.

Our attribution of the competing phase as the AFM phase is justified by NMR data of Tl-2223 – in the phase diagram of multi-layered cuprates shown in Fig. 4 of Ref. [26], T_N decreases with increasing doping in the (underdoped) coexistent SC/AFM region. Moreover, our data on the two-layered cuprate Tl-2212 do not show the zero crossover. This is consistent with ultrafast relaxation data on other one- and two-layered cuprates [32–34] where the coexistence phase is not expected, showing that the observation of the zero crossover in Tl-2223 is intrinsic and not an artifact of the experimental setup. For multi-layered cuprates such as Tl-2223, the AFM and SC order may nucleate on different planes, with each of their correlation lengths much larger than the interlayer distance, such that the two orders can penetrate into each other even at zero magnetic field.

This work presents the first ultrafast optical spectroscopy probe of the coexistence phase in a multi-layered cuprate superconductor where, in zero magnetic field, a new order competes with superconductivity, namely antiferromagnetism. This competing order is intrinsic to the material, is not induced by any external applied field, opens up a QP gap, and is consistent with a commensurate AFM order. This study once again points to the unique characteristic that high-T_c superconductivity results from the competition between more than one type of order parameter. It provides an insight into the mechanism of strongly correlated superconductivity – the quantum fluctuations around this competing order might be responsible for gluing the electrons into Cooper pairs.

4.3 $(Ba,K)Fe_2As_2$ (BKFA) The recently discovered FeAs-based pnictides [35–38] constitute the only class of

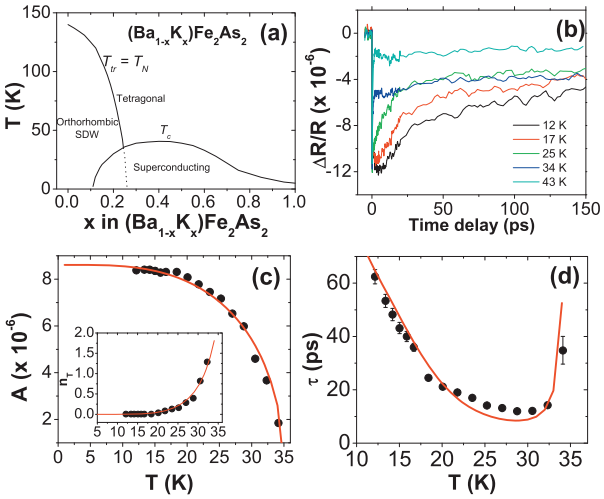

Figure 5 (online colour at: www.pss-rapid.com) (a) Phase diagram of BKFA, with T_c and structural phase transition temperature (T_{tr}) (adapted from [45]). T_N coincides with T_{tr} until both are suppressed [49]. (b) $\Delta R/R$ versus pump–probe delay of optimally doped BKFA ($T_c \sim 36$ K). (c) Amplitude $A(T)$ extracted from single-exponential decay fits. Inset: Density of thermally-excited QPs, $n_T(T)$. Solid lines are fits to the RT model. (d) Relaxation time $\tau(T)$. Solid line is the fit to the RT model (reproduced with permission from [11], http://link.aps.org/abstract/PRL/v104/i2/e027003). Copyright 2007 by the American Physical Society.

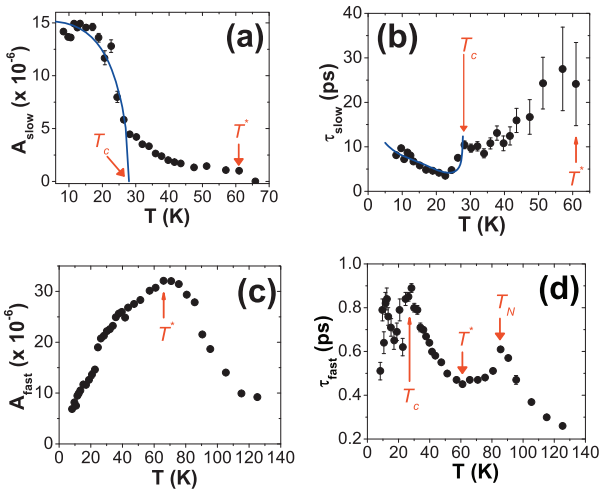

Figure 6 (online colour at: www.pss-rapid.com) For underdoped BKFA ($T_c \sim 28$ K), (a) $A_{slow}(T)$, (b) $\tau_{slow}(T)$, (c) $A_{fast}(T)$, and (d) $\tau_{fast}(T)$, extracted from $\Delta R/R$. In (a), beyond T^*, the slow component disappears. The solid lines in (a) and (b) are fits using the RT model. Taken from Ref. [11].

superconductors, besides the cuprates, with T_c exceeding 50 K. The pnictides have a layered structure like the cuprates, with FeAs planes instead of CuO_2 planes. Like many other superconductors on the border of magnetism, such as the organics [39], heavy-fermions [40], and cuprate HTSCs [41–43], the pnictides exhibit a rich phase diagram, with antiferromagnetism (or SDW) at low dopings [44] and superconductivity at intermediate dopings. Figure 5(a) shows the phase diagram of a particular family of pnictides – the double-layered (Ba,K)Fe_2As_2 (BKFA) family [45]. In the underdoped compound, SDW and SC/normal state regions are mesoscopically separated [46]. Moreover, inelastic neutron scattering in an optimally-doped BKFA revealed the presence of a 14 meV magnetic resonance mode in the SC phase, localized in both energy and wavevector [47]. A large Fe-isotope effect was seen in BKFA, suggesting the role played by magnetic fluctuations in superconductivity [48]. In all these classes of superconductors, how these phases interact with one another, and the role of magnetism, are open questions that might help understand superconductivity in these compounds.

Single-crystalline BKFA samples with sizes up to 10 mm × 5 mm × 0.5 mm were grown by high-temperature solution method [50]. The crystals were cleaved to reveal a fresh surface before data were taken. The values of T_c were confirmed by magnetization data using a Quantum Design Magnetic Property Measurement System. No hysteresis loops in magnetization versus field were found, ruling out the presence of ferromagnetic impurities. Figure 5(b) shows $\Delta R/R$ of the almost optimally-doped sample (OPT), $T_c \sim 36$ K, as a function of T. Ignoring the coherent artifact near $t = 0$ and fitting the data to a single exponential, the fitted amplitude $A(T)$ and relaxation time $\tau(T)$ in the SC state are shown in Fig. 5(c) and (d), respectively, together with the fits to $A(T)$ and $\tau(T)$ using the RT model, yielding $\Delta(0) = 3.0 k_B T_c$ and agreeing with the value obtained from photoemission data [51]. The analysis shows that the QP relaxation dynamics in the OPT compound is well described by the presence of a gap in the density of states at the Fermi level.

We now focus on underdoped BKFA ($T_c \sim 28$ K) and demonstrate that this compound exhibits a *competition* between the SC and SDW orders – the SDW order appears at $T_N \sim 85$ K and gets suppressed starting from $T^* \sim 60$ K, far above T_c. $\Delta R/R$ of underdoped BKFA is qualitatively similar to the OPT data shown in Fig. 5(b). However, data from different T ranges require different number of decaying exponentials to fit them [11] – three below T_c, two between T_c and T^*, and one between T^* and T_N. A three-exponential decay in the SC state was also seen in pump–probe data of Sm(O,F)FeAs single crystals [52]. The slow component ($\tau_{slow} \sim 5 – 30$ ps) corresponds to QP recombination across the SC gap, as shown by the BCS-like T dependence of A_{slow} below T_c (Fig. 6(a)) and by the peak in τ_{slow} at T_c (Fig. 6(b)). The identical RT analysis as for the OPT sample yields $\Delta(0) = 3.0 k_B T_c$ (solid lines in Fig. 6(a), (b)). This shows that the opening of the SC gap in the underdoped sample governs the QP recombination by introducing a relaxation bottleneck.

Next, the fast relaxation component ($\tau_{fast} \leq 1$ ps) below $T_N \sim 85$ K bears the signatures of QP relaxation across the SDW gap: the relaxation time τ_{fast} displays a quasi-divergence at T_N (Fig. 6(d)). The values of T_c and T_N in our

underdoped sample are consistent with that in a muon rotation study [53], and are consistent with the phase diagram in Fig. 5(a). Our measurements not only confirm the coexistence of these two order parameters (evidenced by the existence of both the fast and the slow relaxations below T_c), but also uncover *competition* between SDW and superconductivity, as evidenced by the strong suppression of the SDW amplitude (A_{fast}) below T_c (Fig. 6(c)). The close proximity of the SC and SDW regions in underdoped BKFA results in coupling between the SC and SDW order parameters, and causes the latter to be suppressed in the SC state [11]. The suppression of the SDW order parameter in the SC state was also observed in neutron diffraction data of the electron-doped Fe pnictide $Ba(Fe,Co)_2As_2$ [54].

The sensitivity of the pump–probe technique to the presence of SDW order is further reinforced by our study of QP relaxation in the parent compound $BaFe_2As_2$, with a simultaneous SDW and first-order structural phase transition at $T_N \sim 130$ K [38]. Below T_N, the relaxation amplitude follows a BCS-like T dependence down to the lowest T, reflecting the behavior of the SDW order parameter. In the vicinity of T_N, the relaxation time shows a quasi-divergence, which is the signature of the opening of a gap in the density of states at the Fermi level. This, together with earlier work on the itinerant antiferromagnet $UniGa_5$ [17], shows that the pump–probe technique is sensitive to the SDW order. Data from this parent compound thus justify the attribution of the fast relaxation in underdoped BKFA below 85 K (Fig. 6(d)) to the SDW phase, and that the suppression of A_{fast} below T_c (Fig. 6(c)) corresponds to the suppression of the SDW order parameter.

Moreover, unlike the OPT and parent compound, we observe a very slow component ($\tau_{slower} \sim 100$ ps) that is largely T-independent, disappears above T_c, which we at tribute to spin-lattice relaxation. After the initial fast QP relaxation due to electron-phonon coupling (as manifested by τ_{fast}) in the SDW region, the heated phonons then relax by transferring their energy to the spin bath. This relaxation rate $1/\tau_{sl} = g_{sl}/C_{spin}$, where τ_{sl} is the spin-lattice relaxation time, g_{sl} is the spin-lattice coupling strength and C_{spin} is the spin specific heat [55]. Below T_c, the 14 meV magnetic resonance mode appears [47] in the SC region (see Fig. 7(a) and (b)). This mode penetrates into the neighboring SDW regions and renormalizes the imaginary part of the dynamical spin susceptibility $\mathrm{Im}\,\chi(\varepsilon)$. The spin density of states in the SDW regions is given by $N_s(\varepsilon) = -(1/\pi)\,\mathrm{Im}\,\chi(\varepsilon)$. In the SDW regions, above T_c, there is no renormalization of SDW fluctuations, hence $N_s(\varepsilon)$ at low energies is finite. Below T_c, the increase in amplitude of $\mathrm{Im}\,\chi(\varepsilon)$ at the resonance energy removes spectral weight at lower energies, resulting in the depression of $N_s(\varepsilon)$ at low energies (see Fig. 7(c) and (d)). This transfer of spectral weight from lower to higher energies, as the sample enters the the SC state, was observed in inelastic neutron scattering data [47]. Hence C_{spin} decreases, shortening τ_{sl} (= τ_{slower}) to a value that is observable by our technique. This scenario also explains why we do not observe τ_{slower} in the OPT sample – there are no SDW regions to begin with, hence no SDW fluctuations for the magnetic resonance mode to renormalize.

In addition to establishing the competition between SDW and superconductivity, the data in Fig. 6(a)–(d) carry evidence of a *precursor order* that appears at $T^* \sim 60$ K in the normal state of underdoped BKFA. In Fig. 6(a), A_{slow} exhibits a well-defined tail that survives well above T_c, and disappears above T^*. Compare this to A_{slow} of the OPT sample (Fig. 5(c)), where no such tail exists. This suggests that a kind of precursor superconductivity has already existed between T_c and T^*. A tail in the relaxation amplitude, attributed to the pseudogap, was also seen in underdoped $YBa_2Cu_2O_{7-x}$ [13]. Moreover, in addition to a quasi-divergence of τ_{slow} at T_c (Fig. 6(b)), indicative of the opening up of a SC gap, τ_{slow} continues to increase above T_c and peaks at T^*, showing that, at T^*, another QP gap opens up at the Fermi level. Compare this to a typical superconductor, where τ_{slow} plunges to the metallic value of ~0.5 ps immediately after T_c, and remains almost T-independent above T_c.

Further evidence for precursor pairing at T^* comes from the T dependence of A_{fast} – the SDW amplitude. In the cuprate HTSCs, the proximity of d-wave superconductivity to antiferromagnetism is simply assumed as an experimental fact. However, from a microscopic point of view, d-wave superconductivity in the cuprates turns out to be the winner of the competition between these two orders [56] – this statement may also hold for the extended $s_{\pm}$ pairing that the pnictide superconductors are thought to have, where the gaps at the hole and electron pockets are of *opposite* signs to each other [57]. In the underdoped sample, if a precursor order develops at T^*, the SC fluctuations associated with the precursor order will start to "win over",

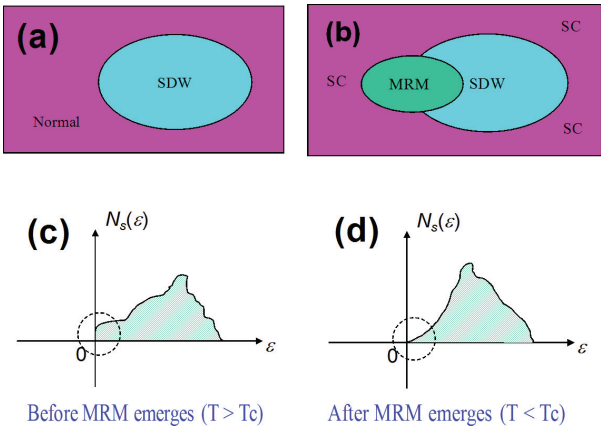

Figure 7 (online colour at: www.pss-rapid.com) Schematics for the existence of the third relaxation process in underdoped BKFA. (a) Normal and SDW phases ($T_c < T < T_N$). (b) Appearance of the magnetic resonance mode (MRM) in the SC state ($T < T_c$). (c) Finite spin density of states, $N_s(\varepsilon)$, at low energies ε, for $T_c < T < T_N$. (d) In the SC state, the imaginary part of the spin susceptibility becomes renormalized, resulting in the suppression of $N_s(\varepsilon)$ at low ε.

i.e. suppress, SDW even in the normal state. This would explain the suppression of A_{fast} below T^* in the underdoped sample (Fig. 6(c)). The rather broad peak in τ_{slow} at T^* might indicate the presence of disorder. It implies that, though the precursor order develops at T^*, disorder may cause the QP excitations to be partially gapless.

Recent photoemission data offered evidence of precursor pairing in the iron pnictide superconductors, such as in La(O,F)FeAs [58, 59] and Sm(O,F)FeAs [60]. The Nernst effect in La(O,F)FeAs also suggested the presence of a "precursor state" between T_c and 50 K in which magnetic fluctuations are strongly suppressed [61]. A recent pump–probe study of Sm(O,F)FeAs gave evidence of a pseudogap-like feature with an onset around 200 K [52]. In the case of BKFA, the precursor order is associated with an intermediate energy scale T^* between magnetism and superconductivity. This precursor order does not compete with superconductivity, but competes with the SDW order. The precursor order that sets in at T^* seems to be intimately related to superconductivity, as its signature becomes the signature of superconductivity below T_c. Therefore, the precursor order may be a precursor of the SC order, much like the Cooper pairing without phase coherence that precedes macroscopic superconductivity in cuprate HTSCs. The detailed nature of the precursor order, whether it is due to phase fluctuations [56] or their interplay with disorder, remains an open scientific question.

5 Conclusions and outlook By taking examples from the cuprates and iron pnictides, we have shown that the ultrafast pump–probe technique can disentangle, via the time domain, the photoinduced QP dynamics of SDW, superconducting, and pseudogap phases, thus allowing us to elucidate possible interactions among these phases. The next steps would be to take THz-TDS and OPTP data on single-crystal or thin-film versions of these samples, to extract the complex optical conductivity $\tilde{\sigma}(\omega,t) = \sigma_1(\omega,t) + i\sigma_2(\omega,t)$, where ω lies in the THz range, and t is the time after photoexcitation for OPTP. From it, we can see how the QPs (related to σ_1) and the SC condensate (related to σ_2) are affected by the presence of other long-range orders in close proximity.

Acknowledgements This work was supported by the Singapore Ministry of Education AcRF Tier 1 (RG41/07) and Tier 2 (ARC23/08) grants, National Research Foundation of Singapore (NRF-CRP4-2008-04) grant, LANL LDRD program, and LANL Center for Integrated Nanotechnologies. This paper is written in memory of the late Professor Sung-Ik Lee.

References

[1] R. D. Averitt and A. J. Taylor, J. Phys.: Condens. Matter **14**, R1357 (2002).
[2] J. Demsar, J. L. Sarrao, and A. J. Taylor, J. Phys.: Condens. Matter **18**, R281 (2006).
[3] D. Talbayev, K. S. Burch, E. E. M. Chia, S. A. Trugman, J. X. Zhu, E. D. Bauer, J. A. Kennison, J. N. Mitchell, J. D. Thompson, J. L. Sarrao, and A. J. Taylor, Phys. Rev. Lett. **104**, 227002 (2010).
[4] P. B. Allen, Phys. Rev. Lett. **59**, 1460 (1987).
[5] S. D. Brorson, A. Kazeroonian, J. S. Moodera, D. W. Face, T. K. Cheng, E. P. Ippen, M. S. Dresselhaus, and G. Dresselhaus, Phys. Rev. Lett. **64**, 2172 (1990).
[6] J. Demsar, B. Podobnik, V. V. Kabanov, T. Wolf, and D. Mihailovic, Phys. Rev. Lett. **82**, 4918 (1999).
[7] J. Demsar, R. D. Averitt, A. J. Taylor, V. Kabanov, W. N. Kang, H. J. Kim, E. Choi, and S. I. Lee, Phys. Rev. Lett. **91**, 267002 (2003).
[8] L. Perfetti, P. A. Loukakos, M. Lisowski, U. Bovensiepen, H. Eisaki, and M. Wolf, Phys. Rev. Lett. **99**, 197001 (2007).
[9] T. Dahm, V. Hinkov, S. V. Borisenko, A. A. Kordyuk, V. B. Zabolotnyy, J. Fink, B. Büchner, D. J. Scalapino, W. Hanke, and B. Keimer, Nature Phys. **5**, 217 (2009).
[10] E. E. M. Chia, J. X. Zhu, D. Talbayev, R. D. Averitt, A. J. Taylor, K. H. Oh, I. S. Jo, and S. I. Lee, Phys. Rev. Lett. **99**, 147008 (2007).
[11] E. E. M. Chia, D. Talbayev, J. X. Zhu, H. Q. Yuan, T. Park, J. D. Thompson, C. Panagopoulos, G. F. Chen, J. L. Luo, N. L. Wang, and A. J. Taylor, Phys. Rev. Lett. **104**, 027003 (2010).
[12] R. H. M. Groeneveld, R. Sprik, and A. Lagendijk, Phys. Rev. B **51**, 11433 (1995).
[13] V. V. Kabanov, J. Demsar, B. Podobnik, and D. Mihailovic, Phys. Rev. B **59**, 1497 (1999).
[14] A. Rothwarf and B. N. Taylor, Phys. Rev. Lett. **19**, 27 (1967).
[15] J. Demsar, V. K. Thorsmølle, J. L. Sarrao, and A. J. Taylor, Phys. Rev. Lett. **96**, 037401 (2006).
[16] V. V. Kabanov, J. Demsar, and D. Mihailovic, Phys. Rev. Lett. **95**, 147002 (2005).
[17] E. E. M. Chia, J. X. Zhu, H. J. Lee, N. Hur, N. O. Moreno, E. D. Bauer, T. Durakiewicz, R. D. Averitt, J. L. Sarrao, and A. J. Taylor, Phys. Rev. B **74**, 140409(R) (2006).
[18] T. Timusk and B. Statt, Rep. Prog. Phys. **62**(1), 61 (1999).
[19] Ø. Fischer, M. Kugler, I. Maggio-Aprile, C. Berthod, and C. Renner, Rev. Mod. Phys. **79**, 353 (2007).
[20] C. Panagopoulos and T. Xiang, Phys. Rev. Lett. **81**, 2336 (1998).
[21] D. Dvorsek, V. V. Kabanov, J. Demsar, S. M. Kazakov, J. Karpinski, and D. Mihailovic, Phys. Rev. B **66**, 020510(R) (2002).
[22] S. C. Zhang, Science **275**, 1089 (1997).
[23] D. P. Arovas, A. J. Berlinsky, C. Kallin, and S. C. Zhang, Phys. Rev. Lett. **79**, 2871 (1997).
[24] Y. S. Lee, R. J. Birgeneau, M. A. Kastner, Y. Endoh, S. Wakimoto, K. Yamada, R. W. Erwin, S. H. Lee, and G. Shirane, Phys. Rev. B **60**, 3643 (1999).
[25] B. Lake, H. M. Ronnow, N. B. Christensen, G. Aeppli, K. Lefmann, D. F. McMorrow, P. Vorderwisch, P. Smelbidl, N. Mangkorntong, T. Sasagawa, M. Nohara, H. Takagi, and T. E. Mason, Nature **415**, 299 (2002).
[26] H. Mukuda, M. Abe, Y. Araki, Y. Kitaoka, K. Tokiwa, T. Watanabe, A. Iyo, H. Kito, and Y. Tanaka, Phys. Rev. Lett. **96**, 087001 (2006).
[27] S. H. Pan, J. P. O'Neal, R. L. Badzey, C. Chamon, H. Ding, J. R. Engelbercht, Z. Wang, H. Eisaki, S. Uchida, A. K. Gupta, K. W. Ng, E. W. Hudson, K. M. Lang, and J. C. Davis, Nature **413**, 282 (2001).

[28] H. J. Kang, P. Dai, J. W. Lynn, M. Matsuura, J. R. Thompson, S. C. Zhang, D. N. Argyriou, Y. Onose, and Y. Tokura, Nature **423**, 522 (2003).
[29] H. Kotegawa, Y. Tokunaga, Y. Araki, G. Q. Zheng, Y. Kitaoka, K. Tokiwa, K. Ito, T. Watanabe, A. Iyo, Y. Tanaka, and H. Ihara, Phys. Rev. B **69**, 014501 (2004).
[30] H. J. Kim, P. Chowdury, S. K. Gupta, N. H. Dan, and S. I. Lee, Phys. Rev. B **70**, 144510 (2004).
[31] J. X. Zhu, W. Kim, C. S. Ting, and J. P. Carbotte, Phys. Rev. Lett. **87**, 197001 (2001).
[32] S. G. Han, Z. V. Vardeny, K. S. Wong, O. G. Symko, and G. Koren, Phys. Rev. Lett. **65**, 2708 (1990).
[33] P. Gay, D. C. Smith, C. J. Stevens, C. Chen, G. Yang, S. J. Abell, D. Z. Wang, J. H. Wang, Z. F. Ren, and J. F. Ryan, J. Low Temp. Phys. **117**, 1025 (1999).
[34] D. C. Smith, P. Gay, D. Z. Wang, J. H. Wang, Z. F. Ren, and J. F. Ryan, Physica C **341–348**, 2219 (2000).
[35] Y. Kamihara, T. Watanabe, M. Hirano, and H. Hosono, J. Am. Chem. Soc. **130**, 3296 (2008).
[36] X. H. Chen, T. Wu, G. Wu, R. H. Liu, H. Chen, and D. F. Fang, Nature **453**, 761 (2008).
[37] N. Ni, S. L. Bud'ko, A. Kreyssig, S. Nandi, G. E. Rustan, A. I. Goldman, S. Gupta, J. D. Corbett, A. Kracher, and P. C. Canfield, Phys. Rev. B **78**, 014507 (2008).
[38] M. Rotter, M. Tegel, and D. Johrendt, Phys. Rev. Lett. **101**, 107006 (2008).
[39] J. Moser, M. Gabay, P. Auban-Senzier, D. Jerome, K. Bechgaard, and J. M. Fabre, Eur. Phys. J. B **1**, 39 (1998).
[40] N. D. Mathur, F. M. Grosche, S. R. Julian, I. R. Walker, D. M. Freye, R. K. W. Haselwimmer, and G. G. Lonzarich, Nature **394**, 39 (1998).
[41] S. A. Kivelson, I. P. Bindloss, E. Fradkin, V. Oganesyan, J. M. Tranquada, A. Kapitulnik, and C. Howald, Rev. Mod. Phys. **75**, 1201 (2003).
[42] S. Sachdev, Rev. Mod. Phys. **75**, 913 (2003).
[43] S. Hüfner, M. A. Hossain, A. Damascelli, and G. A. Sawatzky, Rep. Prog. Phys. **71**, 062501 (2008).
[44] C. de la Cruz, Q. Huang, J. W. Lynn, J. Li, W. R. II, J. L. Zarestky, H. A. Mook, G. F. Chen, J. L. Luo, N. L. Wang, and P. Dai, Nature **453**, 899 (2008).
[45] M. Rotter, M. Pangerl, M. Tegel, and D. Johrendt, Angew. Chem. Int. Ed. **47**, 7949 (2008).
[46] J. T. Park, D. S. Inosov, C. Niedermayer, G. L. Sun, D. Haug, N. B. Christensen, R. Dinnebier, A. V. Boris, A. J. Drew, L. Schulz, T. Shapoval, U. Wolff, V. Neu, X. Yang, C. T. Lin, B. Keimer, and V. Hinkov, Phys. Rev. Lett. **102**, 117006 (2009).
[47] A. D. Christianson, E. A. Goremychkin, R. Osborn, S. Rosenkranz, M. D. Lumsden, C. D. Malliakas, I. S. Todorov, H. Claus, D. Y. Chung, M. G. Kanatzidis, R. I. Bewley, and T. Guidi, Nature **456**, 930 (2008).
[48] R. H. Liu, T. Wu, G. Wu, H. Chen, X. F. Wang, Y. L. Xie, J. J. Yong, Y. J. Yan, Q. J. Li, B. C. Shi, W. S. Chu, Z. Y. Wu, and X. H. Chen, Nature **459**, 64 (2009).
[49] H. Chen, Y. Ren, Y. Qiu, W. Bao, R. H. Liu, G. Wu, T. Wu, Y. L. Xie, X. F. Wang, Q. Huang, and X. H. Chen, Europhys. Lett. **85**, 17006 (2009).
[50] G. F. Chen, Z. Li, J. Dong, G. Li, W. Z. Hu, X. D. Zhang, X. H. Song, P. Zheng, N. L. Wang, and J. L. Luo, Phys. Rev. B **78**, 224512 (2008).
[51] H. Ding, P. Richard, K. Nakayama, T. Sugawara, T. Arakane, Y. Sekiba, A. Takayama, S. Souma, T. Sato, T. Takahashi, Z. Wang, X. Dai, Z. Fang, G. F. Chen, J. L. Luo, and N. L. Wang, Europhys. Lett. **83**, 47001 (2008).
[52] T. Mertelj, V. V. Kabanov, C. Gadermaier, J. Karpinski, and D. Mihailovic, Phys. Rev. Lett. **102**, 117002 (2009).
[53] A. A. Aczel, E. Baggio-Saitovitch, S. L. Budko, P. C. Canfield, J. P. Carlo, G. F. Chen, P. Dai, T. Goko, W. Z. Hu, G. M. Luke, J. L. Luo, N. Ni, D. R. Sanchez-Candela, F. F. Tafti, N. L. Wang, T. J. Williams, W. Yu, and Y. J. Uemura, Phys. Rev. B **78**, 214503 (2008).
[54] D. K. Pratt, W. Tian, A. Kreyssig, J. L. Zarestky, S. Nandi, N. Ni, S. L. Bud'ko, P. C. Canfield, A. I. Goldman, and R. J. McQueeney, Phys. Rev. Lett. **103**, 087001 (2009).
[55] R. D. Averitt, A. I. Lobad, C. Kwon, S. A. Trugman, V. K. Thorsmølle, and A. J. Taylor, Phys. Rev. Lett. **87**, 017401 (2001).
[56] P. A. Lee, N. Nagaosa, and X. G. Wen, Rev. Mod. Phys. **78**, 17 (2006).
[57] I. I. Mazin, D. J. Singh, M. D. Johannes, and M. H. Du, Phys. Rev. Lett. **101**, 057003 (2008).
[58] T. Sato, S. Souma, K. Nakayama, K. Terashima, K. Sugawara, T. Takahashi, Y. Kamihara, M. Hirano, and H. Hosono, J. Phys. Soc. Jpn. **77**, 063708 (2008).
[59] Y. Ishida, T. Shimojima, K. Ishizaka, T. Kiss, M. Okawa, T. Togashi, S. Watanabe, X. Y. Wang, C. T. Chen, Y. Kamihara, M. Hirano, H. Hosono, and S. Shin, Phys. Rev. B **79**, 060503(R) (2009).
[60] H. Y. Liu, X. W. Jia, W. T. Zhang, L. Zhao, J. Q. Meng, G. D. Liu, X. L. Dong, G. Wu, R. H. Liu, X. H. Chen, Z. A. Ren, W. Yi, G. C. Che, G. F. Chen, and N. L. Wang, Chin. Phys. Lett. **25**, 3761 (2008).
[61] Z. W. Zhu, Z. A. Xu, X. Lin, G. H. Cao, C. M. Feng, G. F. Chen, Z. Li, J. L. Luo, and N. L. Wang, New J. Phys. **10**, 063021 (2008).